

Heteroepitaxial Growth of a Zeolite**

Tatsuya Okubo,* Toru Wakihara, Jacques Plévert, Sankar Nair, Michael Tsapatsis, Yoshifumi Ogawa, Hiroshi Komiyama, Masahiro Yoshimura, and Mark E. Davis

Zeolites contain molecular-sized void spaces within their crystal structures.^[1] Over 120 framework topologies have been recognized for zeolites and related materials.^[2] Because of their unique structures, zeolites and related microporous materials have been investigated as hosts for molecules, ions, and clusters, and interesting phenomena have been reported, especially for optical applications.^[3] The ability to provide for the heterogeneous connection of zeolite structures may enable the construction of multidimensional, nanospacial networks. Such nanospacial networks may serve as hosts to integrate molecular electronics and other molecular devices within the structures. Here we take the first step toward this goal by connecting one-dimensional cancrinite channels with zero-dimensional sodalite cages.

Certain zeolites are composed of the same building units but with different layer-stacking sequences.^[1] Thus far, such "intergrowth" phenomena have been investigated with micrometer-sized crystals such as ERI/OFF,^[4] MFI/MEL,^[5] FAU/EMT,^[6] and others.^[7–9] Recently, designed overgrowth for EMT/FAU on a micrometer scale was reported.^[10] To move from observations on a micrometer scale to applications that require control over larger length scales, such as optical devices, we focused on the construction of the first heterogeneous connection between two zeolites on a millimeter scale.

Zeolites composed of six-membered rings proved to be useful for the construction of multidimensional, nanospacial networks. Sodalite and cancrinite have structural similarities, since their aluminosilicate layers of six-membered rings are identical to each other, and the structures only differ in the stacking sequences of these layers (Figure 1). The ABCABC

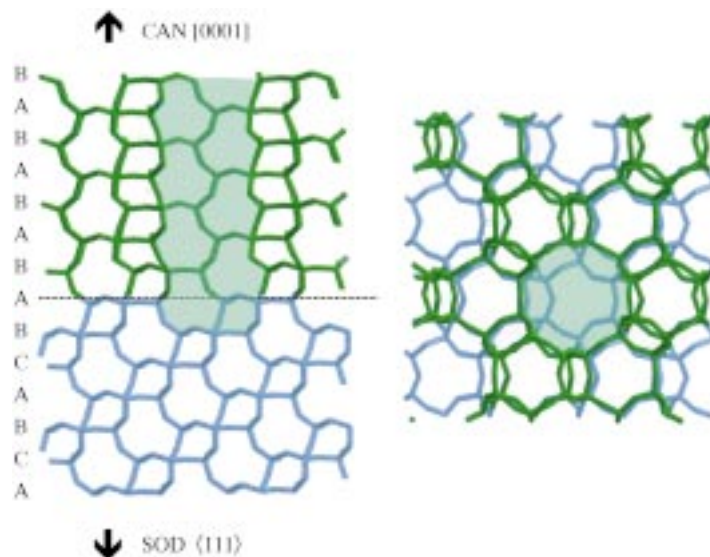


Figure 1. A model of heteroepitaxial growth of cancrinite on sodalite. The stacking sequence along the cancrinite [0001] direction is ABABAB (top), and that along the sodalite $\langle 111 \rangle$ direction is ABCABC (bottom). A composite view down the cancrinite [0001]/sodalite $\langle 111 \rangle$ direction is shown on the right. The shaded areas represent the connection of a sodalite cage and a 12-membered ring cancrinite channel on the left, and a single sodalite cage on the right.

- [*] Prof. Dr. T. Okubo
PRESTO, Japan Science and Technology Corporation (JST)
and
Department of Chemical System Engineering
The University of Tokyo
Bunkyo-ku, Tokyo 113-8656 (Japan)
Fax: (+81)3-5800-3806
E-mail: okubo@chemsys.t.u-tokyo.ac.jp
T. Wakihara, Dr. J. Plévert,^[+] Y. Ogawa, Prof. Dr. H. Komiyama
Department of Chemical System Engineering
The University of Tokyo
S. Nair, Prof. Dr. M. Tsapatsis
Department of Chemical Engineering, University of Massachusetts
Amherst, MA 01003 (USA)
Prof. Dr. M. Yoshimura
Materials and Structures Laboratory, Tokyo Institute of Technology
Midori, Yokohama 226-8503 (Japan)
Prof. Dr. M. E. Davis
Chemical Engineering, California Institute of Technology
Pasadena, CA 91125 (USA)

- [+] Present address:
Department of Chemistry and Biochemistry, Arizona State University
Tempe, AZ 85287-1604 (USA)

- [**] T.W. and T.O. are grateful to H. Tsunakawa of the High Voltage Electron Microscope Laboratory, University of Tokyo (UT), and Prof. Y. Ikuhara, Engineering Research Institute, UT, for the 400-kV SAED experiments and their analyses, respectively. H. Shiga, T. Hayashi and T. Shiraki are acknowledged for preliminary experiments. This work was supported by a Grant-in-Aid for Scientific Research from the Ministry of Education, Science, Sports and Culture and the TEPCO Foundation.

sequence generates sodalite cages, while the ABABAB sequence results in the one-dimensional 12-membered ring cancrinite channels that run along the direction perpendicular to the layer.^[1, 9] The ABCABC and ABABAB sequences are along the sodalite $\langle 111 \rangle$ axis and the cancrinite [0001] axis, respectively. The structural similarity enables us to connect these crystals in a heteroepitaxial manner. The concept of designed heteroepitaxial connectivity is not limited to the system demonstrated here; for example, other three-dimensional void spaces could be formed by controlling the stacking sequences from zeolites such as AABBC for chabazite, AABAAB for offretite, AABAAC for erionite, AABAABB for gmelinite, etc.

Millimeter-sized cubic sodalite crystals were synthesized at 973 K and about 80 MPa from a reaction mixture of composition $3\text{SiO}_2:3\text{Al}:2\text{NaCl}:9\text{NaOH}:97\text{H}_2\text{O}$.^[11] The optical micrograph of a single crystal thus obtained is shown in Figure 2. The shape of the single crystals is a rhombic dodecahedron. A crystal with dodecahedral habit is expected to have $\{110\}$ faces. The rhombus faces were verified to have $\{110\}$ orientations by back reflection Laue X-ray photography.^[11a] Cancrinite was synthesized as described in the Experimental Section. When no sodalite crystals are added, aggregates of cancrinite crystals in the shape of hexagonal prisms are precipitated. The conditions necessary for heteroepitaxial growth of cancrinite on a sodalite substrate were

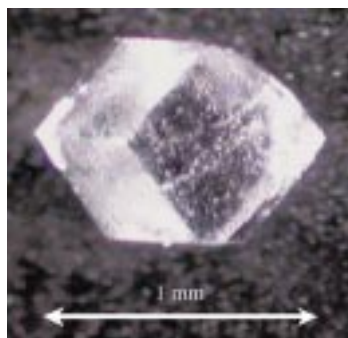


Figure 2. Optical photograph of a millimeter-sized sodalite single crystal grown under high-temperature, high-pressure hydrothermal conditions. The shape of the sodalite crystal is a dodecahedron, and the rhombus faces are sodalite {110} planes.

optimized by reducing the contribution of spontaneous nucleation. Such conditions were found by varying the time at which the sodalite crystals were introduced into the cancrinite synthesis solution. Millimeter-sized sodalite single crystals, prepared separately as described above, were placed in the cancrinite synthesis solution in the middle of the heating period. After a certain time, sodalite crystals overgrown with cancrinite were recovered and washed with distilled water. The changes in the morphology on sodalite faces were observed with a powder X-ray diffractometer (PXRD, Mac Science, MO3XHF²²), a field-emission scanning electron microscope (FE-SEM, Hitachi S-900), and transmission electron microscopes (TEM, JEOL JEM 2010F and JEM 4000FX-II) as a function of the cancrinite synthesis time. For the TEM observations, the sample was processed with a focused ion beam system (FIB, Micrion, JFIB-2100). A cross-sectional specimen was prepared and thinned down by a gallium ion beam to only 200 nm, since the zeolite framework proved to be fragile at lower thickness. In addition to as-grown {110} faces, sodalite {111} surfaces were prepared by mechanical polishing.

By trial and error, conditions for shaping the surface topology were found for the sodalite faces. Typical synthesis conditions are summarized in Table 1. The best results were obtained when cancrinite was grown on a sodalite substrate

Table 1. Typical conditions for cancrinite heteroepitaxial growth on sodalite substrates (see Experimental Section).

Entry	Aging (at 298 K)	Preheating (at 358 K)	Growth (at 358 K)
1	2 h	18 h	48 h
2	2 h	16 h	48 h

for 48 h after preheating the cancrinite synthesis solution for 18 h at 358 K (entry 1). The single crystals were placed in the cancrinite synthesis vessel after the spontaneous nucleation and the greater part of crystal growth had been completed. An FE-SEM photograph of the synthesis product on a millimeter-sized sodalite {110} substrate is shown in Figure 3. This figure shows the formation of nanocrystals of cancrinite, identified by PXRD, with regular hexagonal-prism shape. The crystals are homogeneous in size, and the length-to-diameter ratio is relatively constant. Apparently, the supersaturation in the

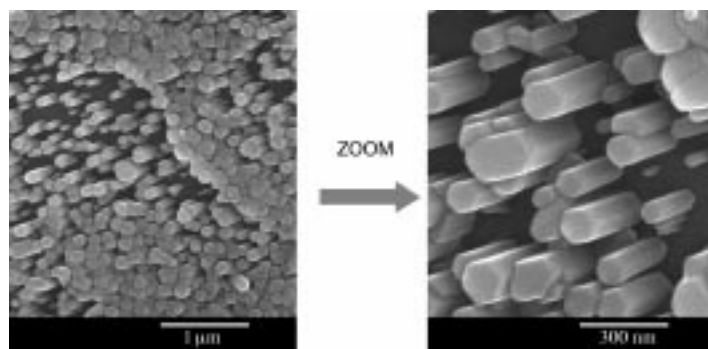


Figure 3. FE-SEM photographs of synthesis products on a sodalite {110} substrate. The cancrinite crystals in the shape of hexagonal prisms grow in parallel and have the same orientation in the basal plane.

synthesis medium was low enough to allow the formation of well-faceted crystals. The growth rate in the pore direction was higher than that in the basal plane of cancrinite, and this resulted in crystals with a nearly prismatic shape. The crystals grow in parallel and have the same orientation in the basal plane. In particular, the main axis of the crystals growing on sodalite {111} faces should be perpendicular to the substrate, while the crystals growing on the {110} faces should be inclined with a constant tilt angle of around 35°. This angle corresponds to that between the [011] and [111] directions in cubic crystal. These results strongly support epitaxial growth of cancrinite crystals on sodalite crystal surfaces.

The orientation of cancrinite crystals, synthesized under the conditions of entry 1 in Table 1, was determined by examining cross sections of the sodalite substrate by TEM. As soon as the focus and the astigmatism were adjusted, TEM photographs and SAED patterns were recorded under low-dose conditions to avoid destroying the crystal structure. The results revealed that the cancrinite grew heteroepitaxially on the sodalite substrate. A TEM photograph of the cross section of the sodalite {111} plane is shown in Figure 4a. Dense and well-aligned cancrinite crystals grow perpendicularly to the substrate surface with height of around 200 nm. SAED patterns in the sodalite region, apart from the overgrown layer, are taken along the $[1\bar{2}\bar{5}]$ zone axis. All the spots can be indexed with the cubic unit cell of sodalite. On shifting the beam spot toward the cancrinite region, while keeping all conditions unchanged, weak spots were detected among the strong spots of the cubic structure (Figure 4b). The new spots can be indexed to the $[2\bar{1}12]$ zone axis. A composite electron-diffraction simulation along the sodalite $[1\bar{2}\bar{5}]$ /cancrinite $[2\bar{1}12]$ zone axis is shown in Figure 4c. All the spots in Figure 4b correspond well with the simulated results in Figure 4c. The superposition of spots of both structures reveals the coincidence of planes $(1\bar{2}1)_{\text{SOD}}//(\text{O}1\bar{1}\text{O})_{\text{CAN}}$ and $(210)_{\text{SOD}}//(\text{2}\bar{1}\bar{1}\text{1})_{\text{CAN}}$. The following orientation relationships between the two systems are obtained: cubic(111)//hexagonal(0001), cubic($1\bar{2}1$)//hexagonal($\text{O}1\bar{1}\text{O}$), cubic($2\bar{1}\bar{1}$)//hexagonal($10\bar{1}\text{O}$). The unit-cell orientation relationships correspond to the epitaxial overgrowth of cancrinite crystals on the sodalite substrate, as shown in Figure 1.

Here we showed that the heteroepitaxial growth of cancrinite on millimeter-sized sodalite single crystals has

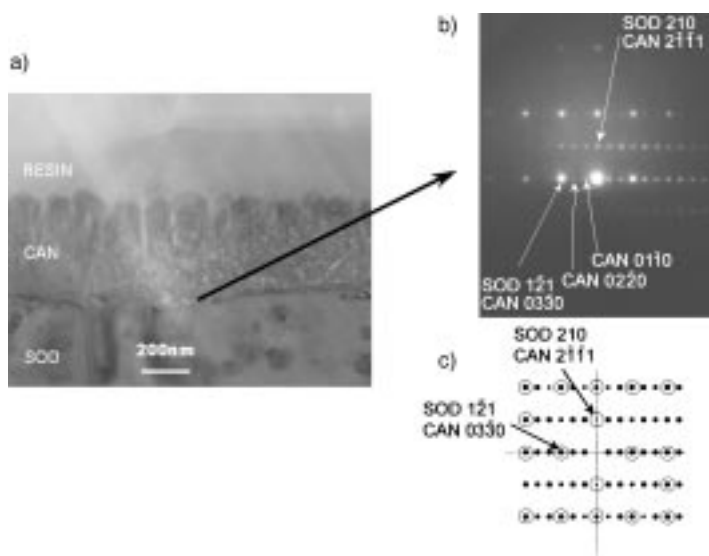


Figure 4. A TEM photograph and an SAED pattern of a cross section of a layer overgrown on a sodalite [111] substrate. a) The substrate is sodalite [111] prepared by mechanical polishing. The cancrinite crystals grow perpendicular to the sodalite [111] substrate. b) An SAED pattern recorded along the sodalite [125] zone axis. Spots due to cancrinite and sodalite are observed and indexed. c) A composite electron-diffraction simulation along the sodalite [125]/cancrinite [2112] zone axis. The spots resulting from superposition of diffracted beams from sodalite and cancrinite crystal planes are circled.

been accomplished. To the best of our knowledge, these results are the first to show the feasibility of preparing in-plane and out-of-plane oriented zeolite films with channels perpendicular to the substrate. These composite structures suggest a pathway toward the fabrication of multidimensional, nanospatial networks.

Experimental Section

The synthesis consists of aging, preheating without sodalite substrates, and growth with sodalite substrates. The starting solution had the composition $34\text{SiO}_2:2\text{Al}:50\text{NaNO}_3:200\text{NaOH}:2000\text{H}_2\text{O}$. First, aluminum powder, $0.1\ \mu\text{m}$ in size, was added to a concentrated solution of NaOH in a Teflon vessel and dissolved completely. In another Teflon vessel, SiO_2 (Cab-O-Sil M-5), NaNO_3 , and the remaining NaOH and distilled water were mixed until the solution became transparent. Then the former solution was added to the latter, and the mixed clear solution was stirred for 2 h. All these procedures were carried out at 298 K. After this aging step, the solution was heated at 358 K for 18 h without sodalite substrates. Then, sodalite was introduced, and the mixture heated at 358 K for 48 h. The product was washed with distilled water and dried at 358 K. When the preheating phase was shortened by 2 h (Entry 2 in Table 1), heterogeneous nucleation on sodalite was enhanced, and a densely accumulated cancrinite layer was formed.

Received: October 2, 2000 [Z15890]

- [1] a) D. W. Breck, *Zeolite Molecular Sieves*, Wiley, New York, **1974**;
 b) R. M. Barrer, *Hydrothermal Chemistry of Zeolites*, Academic Press, London, **1982**.
 [2] a) W. M. Meier, D. H. Olson, C. Baerlocher, *Atlas of Zeolite Structure Types*, 4th revised ed., Butterworth-Heinemann, London, **1996**;
 b) <http://www.iza-structure.org/>.
 [3] a) U. Vietze, O. Krauss, F. Laeri, G. Ihlein, F. Schüth, B. Limberg, M. Abraham, *Phys. Rev. Lett.* **1998**, *21*, 4628–4631; b) G. Ihlein, F. Schüth, O. Krauss, U. Vietze, F. Laeri, *Adv. Mater.* **1998**, *10*, 1117–1119; c) P. Yang, G. Wirnsberger, H. C. Huang, S. R. Cordero, M. D.

- McGhee, B. Scott, T. Deng, G. M. Whitesides, B. F. Chmelka, S. K. Buratto, G. D. Stucky, *Science* **2000**, *287*, 465–467; d) Y. Wada, T. Okubo, M. Ryo, T. Nakazawa, Y. Hasagawa, S. Yanagida, *J. Am. Chem. Soc.* **2000**, *122*, 8583–8584.
 [4] K. P. Lillerud, J. H. Raeder, *Zeolites* **1986**, *6*, 474–483.
 [5] a) J. M. Thomas, G. R. Millward, *J. Chem. Soc. Chem. Commun.* **1982**, 1380–1383; b) G. R. Millward, S. Ramdas, J. M. Thomas, M. T. Barlow, *J. Chem. Soc. Faraday Trans. 2* **1983**, 1075–1082.
 [6] a) E. J. P. Feijen, K. Vadder, M. H. Bosschaerts, J. L. Lievens, J. A. Martens, P. J. Grobet, P. A. Jacobs, *J. Am. Chem. Soc.* **1994**, *116*, 2950–2957; b) M. W. Anderson, K. S. Pachis, F. Prebin, S. W. Carr, O. Terasaki, T. Ohsuna, V. Alfreddson, *J. Chem. Soc. Chem. Commun.* **1991**, 1660–1664.
 [7] C. Weidenthaler, R. X. Fischer, R. D. Shannon, O. Medenbach, *J. Phys. Chem.* **1994**, *98*, 12687–12694.
 [8] S. Nair, L. A. Villaescusa, M. A. Cambor, M. Tsapatsis, *Chem. Commun.* **1999**, 921–922.
 [9] J. Plevért, R. M. Kirchner, R. W. Broach, *Proc. 12th Int. Zeolite Conf. 1988* (Baltimore), Materials Research Society, **1999**, pp. 2445–2452.
 [10] A. M. Goossens, B. H. Wouters, V. Buschmann, J. A. Martens, *Adv. Mater.* **1999**, *11*, 561–564.
 [11] a) T. Shiraki, T. Wakihara, M. Sadakata, M. Yoshimura, T. Okubo, *Microporous Mesoporous Mater.*, in press; b) T. Hayashi, H. Shiga, M. Sadakata, T. Okubo, *J. Mater. Res.* **1998**, *13*, 891–895.

Rotaxane-Encapsulation Enhances the Stability of an Azo Dye, in Solution and when Bonded to Cellulose**

Michael R. Craig, Michael G. Hutchings,
 Tim D. W. Claridge, and Harry L. Anderson*

The groups of Cram and Warmuth have shown that exotic high-energy intermediates such as cyclobutadiene, *ortho*-benzynes, and cycloheptatetraene can be stabilized by encapsulation inside calixarene-based cages.^[1] These results inspired us to attempt to encapsulate and stabilize more mundane species such as dyes^[2] and conjugated polymers^[3] by synthesizing rotaxanes^[4] in which the reactive π system of the dye or polymer is protected inside the cavity of a macrocycle. We have previously reported the synthesis of azo dye rotaxanes;^[2a-c,5] however, two key questions remained unanswered: a) Does encapsulation improve the longevity of the azo chromophore? b) Does encapsulation detrimentally prevent the dye from binding to surfaces? Here we address these issues by reporting an efficient synthesis of a

[*] Dr. H. L. Anderson, M. R. Craig, Dr. T. D. W. Claridge
 Department of Chemistry, Dyson Perrins Laboratory
 University of Oxford
 South Parks Road, Oxford, OX13QY (UK)
 Fax: (+44) 1865-275674
 E-mail: harry.anderson@chem.ox.ac.uk
 Dr. M. G. Hutchings^[†]
 BASF plc
 PO Box 4, Earl Road, Cheadle Hulme, Cheshire, SK8 6QG (UK)

[**] This work was supported by the Engineering and Physical Sciences Research Council (UK) and by BASF plc.

[†] Current address: Dy Star UK Ltd, PO Box 63, Earl Road, Cheadle Hulme, Cheshire, SK8 6GH (UK)

Supporting information for this article is available on the WWW under <http://www.angewandte.com> or from the author.